ISBN: 978-3-95450-261-5 ISSN: 2673-7000 doi: 10.18429/JACoW-NAPAC2025-MOP026

DESIGN OF PHASE DIVERSITY ELECTRO-OPTIC SAMPLING OF THz COHERENT TRANSITION RADIATION

S. J. Kelham*, G. Ha, Northern Illinois University, Dekalb, IL, United States
P. Piot, Argonne National Laboratory, Lemont, IL, United States

Abstract

We report progress on the design of a Phase Diversity Electro-Optic Sampling (DEOS)-based longitudinal profile measurement system. The current design uses THz coherent transition radiation (CTR) to convey the bunch longitudinal information. A 1550 nm fiber laser available at the Argonne Wakefield Accelerator facility will be used as the probe for electro-optic sampling. Specifically, we discuss pulse synchronization and probe beam transport, the design and optimization of the probe beam stretcher, and the design of the probe beam detection system.

INTRODUCTION

Electro-optic sampling (EOS) has emerged as one of the most promising non-invasive diagnostics for characterizing relativistic electron bunches [1–3]. Recent advancement in spectral encoding techniques—particularly the development of Phase-Diversity Electro-Optic Sampling (DEOS) [4]—has enabled single-shot measurements with temporal resolutions at or even below the conventional limit set by probe duration and bandwidth [5]. These advances may enable accurate, high-resolution, non-invasive measurements of bunch profile in the sub-picosecond regime. Such capability could be particularly important for advanced accelerator concepts (AAC) that require various shaped bunches [6, 7].

Such shaped electron bunches for AAC typically have rms bunch lengths of 0.1-10 ps [8, 9], which falls within the range where traditional EOS methods may face resolution limitations. In addition to sub-picosecond bunch lengths, measurement of shaped, non-symmetric electron bunches [10,11], which can be produced by several different ways [12–14], could be a new challenge. These shaped profiles usually include sharp edges, fine structures, or steep gradients.

Efforts are underway to address this challenge in measuring shaped bunch profiles. We are preparing experiments to explore the measurement of shaped bunches using DEOS method. Producing various shaped bunches are rather straightforward at Argonne Wakefield Accelerator (AWA) facility [15]. Thus, as the first step, we are building DEOS system and plan to validate it using CTR from an existing OTR screen on the beamline.

It is worth note that we have designed a similar measurement system with 785 nm photocathode laser as a probe beam source [16]. Here the photocathode laser's bandwidth is limited due to amplification process for intense photoemission. A 3 nm bandwidth of the photocathode laser significantly limits the resolution of the spectral encoding measurement. Also, the system included a free-space motorized delay stage for synchronization between the IR probe beam and the THz CTR. It introduced challenges on alignment and coarse and fine timing synchronization.

In this paper, we present a recent design with a different probe beam source and controls, which can significantly improve the resolution and ease the synchronization. Recently, Menlo Systems 1550 nm fiber laser and RF delay circuit have been successfully implemented at the AWA facility. The delay control of the fiber laser pulse train with respect to the master clock was demonstrated, making the fiber laser as preferred probe beam for the DEOS experiment. To accommodate the new probe laser, the transport, stretcher, and detection line must be redesigned. Figure 1 shows the layout of the current design. We will discuss the design procedure for this new system.

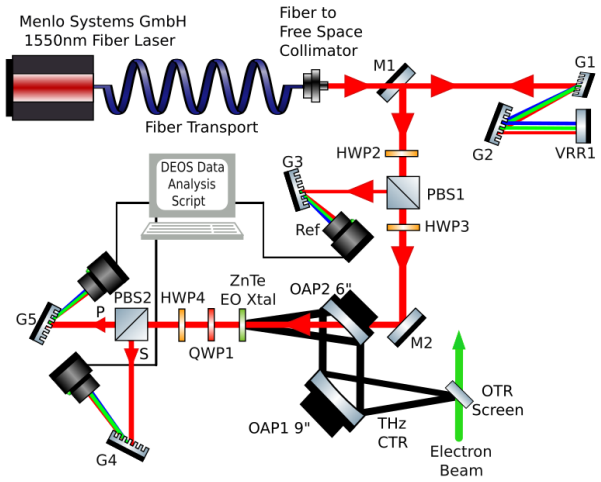

Figure 1: Optics diagram of proposed CTR THz bunch profile monitor. Probe beam is transported by polarization maintaining fibers and dispersion compensating fibers. THz CTR is generated by beam interaction with an OTR screen and focused to a ZnTe crystal using off-axis parabolic mirrors. Unmodulated reference and modulated S and P polarizations will be recorded for DEOS reconstruction.

PROBE BEAM STRETCHER DESIGN FOR 1550 nm FIBER LASER

In a spectral encoding measurement, the probe beam is given a linear frequency chirp to create a time-to-wavelength mapping. The analysis of the probe beam's modulated spectra can return the electron bunch temporal profile. There are various methods for giving the probe beam a frequency chirp, but we have opted for a system of two gratings to act as

* z1904611@students.niu.edu

ISBN: 978-3-95450-261-5 ISSN: 2673-7000 doi: 10.18429/JACoW-NAPAC2025-MOP026

a pulse stretcher. Incident pulse will be at or near its Fourier transform-limited duration (56 fs), so the two-grating system can act as a stretcher providing a negative chirp to the probe beam.

We define the configuration space of the stretcher as the space of possible grating period and incident angle combinations. The number of positive orders m_{pos} and negative orders m_{neg} can be determined by [17],

$$m_{pos} = \left\lceil (1 - \sin(\alpha)) \frac{d}{\lambda_0} \right\rceil,$$
$$m_{neg} = \left\lfloor (-1 - \sin(\alpha)) \frac{d}{\lambda_0} \right\rfloor,$$
$$m_{tot} = 1 + |m_{pos}| + |m_{neg}|, \quad (1)$$

where α is the angle of incidence with respect to the grating normal, d is the grating period, and λ_0 is the laser wavelength. We can use Eq. (1) to search valid configuration space for the design. Stretcher configurations with only the 0th order produce reflection only, which is not suitable for the design. Configurations with more than one diffracted mode are inherently inefficient, and therefore not preferable for the stretcher design.

The Group Velocity Dispersion (GVD) of the incident light pulse is then determined for each point in the valid configuration space using,

$$GVD_{grating} = -\frac{\lambda_0^3}{\pi c^2 d^2} \frac{1}{\cos^2(\beta_m(\lambda_0))}, \quad (2)$$

where $\beta_m(\lambda_0)$ is determined by the grating equation written as,

$$\beta_m(\lambda_0) = \arcsin\left(-\sin(\alpha) + \frac{m\lambda}{d}\right). \quad (3)$$

The diffracted pulse experiences the GVD over the travel distance L_d between G_1 and G_2, resulting in a total Group Delay Dispersion (GDD) that determines the outgoing pulse length (τ). The relation between GDD and τ for the two-grating system is given by,

$$GDD = -\left(\frac{\tau_0}{4 \ln 2}\right) \sqrt{\tau^2 - \tau_0^2}. \quad (4)$$

Therefore, to determine L_d producing the desired τ, we use the following relationship,

$$L_d = \frac{GDD}{GVD}. \quad (5)$$

While the described procedure helps to narrow down the valid region and the required path length between the gratings, many of these configurations are geometrically invalid. In some configurations, the required L_d causes the dispersed probe beam to overfill the grating G_2. In other configurations, $\beta_m(\lambda_0) - \alpha$ is small enough so that G_2 blocks the incident beam. This happens when the configuration is too close to the Littrow condition [17]. Figure 2 shows the valid configuration space after geometric validation, considering only high-dispersion designs [17]. For the wavelength and bandwidth of the fiber laser available at the AWA facility, and for the desired stretched pulse length, the region valid for the design requires $600\frac{g}{\text{mm}}$ diffraction gratings, and the range of possible incident angles (α) is between -17° and -5°.

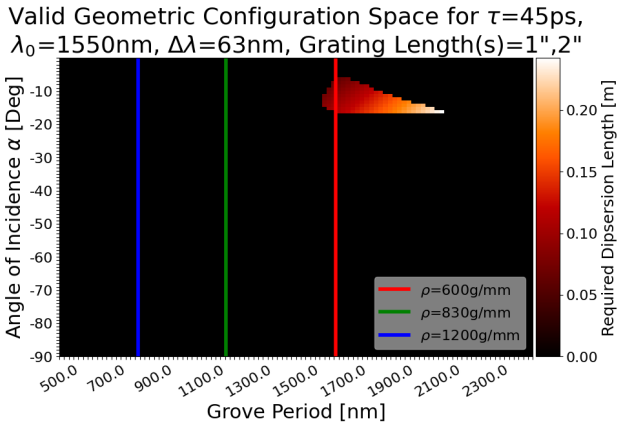

Figure 2: Valid configuration space post-geometric validation.

Geometric validity of this configuration can be visibly observed by generating a schematic of the grating stretcher with the diffracted ray paths using Eq. (3). A layout drawn in Fig. 3 is one of such valid configurations, with $\rho = 600\frac{g}{\text{mm}}$ and $\alpha = -17°$.

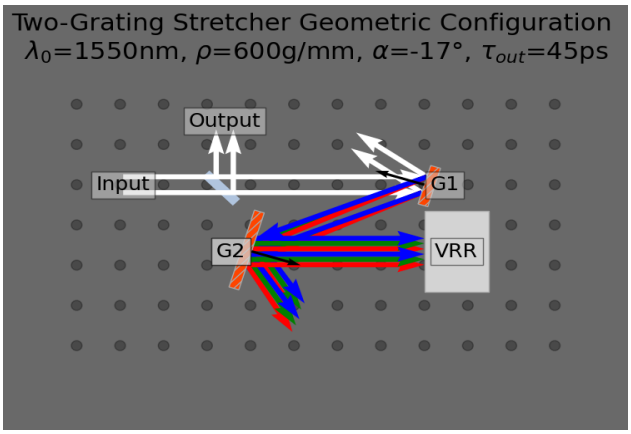

Figure 3: Schematic of valid stretcher configuration drawn to-scale with optics breadboard. α=-17°and $\rho = 600\frac{g}{mm}$.

Finally, it is important for spectral encoding experiments to preserve linear chirp in the probe beam. This can be accomplished by minimizing the higher-order dispersion contributions from the stretcher to the pulse phase, specifically Third-Order Dispersion (TOD). For a two-grating system, the TOD can be expressed as [18],

$$TOD = -\frac{3\lambda}{2\pi c \cos^2(\beta(\lambda_0))} \times \left(\cos^2(\beta(\lambda_0)) + \frac{\lambda_0}{d}\left(\frac{\lambda_0}{d} + \sin(\alpha)\right)\right) \times SOD. \quad (6)$$

ISBN: 978-3-95450-261-5 ISSN: 2673-7000 doi: 10.18429/JACoW-NAPAC2025-MOP026

In Fig. 4, TOD is determined for various α in the acceptable range. The configuration with the smallest higher-order dispersion term is the -17°configuration, which is the one shown in Fig. 3.

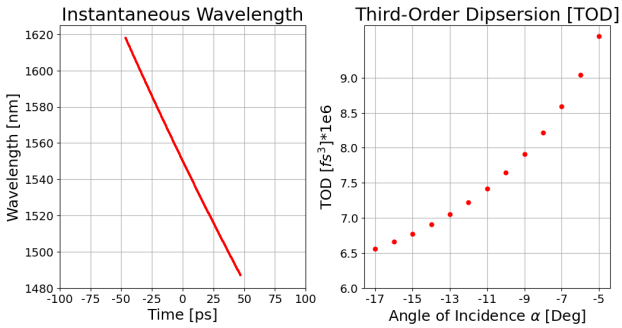

Figure 4: Time-to-Wavelength mapping and TOD for valid α. The ideal configuration for linear chirp is with α=-17°. The Time-to-Wavelength mapping for the outgoing stretched pulse is displayed.

SIMULATION OF DEOS-BASED RECONSTRUCTION OF GAUSSIAN BEAM WITH 1550 nm PROBE BEAM IN ZnTe CRYSTAL

The phase retardance ($\Delta\phi(t)$) is obtained by propagating the CTR pulse through the ZnTe electro-optic crystal [1] in the simulation script, while accounting for the mismatch between probe beam group velocity and the CTR radiation's phase velocities.

The computed phase retardance is applied to modulate the time-dependent intensity profiles of the pre-stretched beam, thereby determining the intensity spectrum. The time-to-Wavelength mapping obtained in Fig. 4 is then used to convert the intensity spectrum of both polarizations into equivalent time (t_{eq}). the intensity spectrums in combination with an unmodulated reference spectrum is used to determine the Electro-Optic signals $Y_1(t_{eq})$ and $Y_2(t_{eq})$ [4]. The THz electric field from the CTR pulse is subsequently retrieved using the maximum-ratio combining method [4] with $\widetilde{Y}_1(\Omega)$, $\widetilde{Y}_2(\Omega)$, and the Fourier-domain transfer functions [4]. The simulation shown in Fig. 5 shows the reconstruction the electron beam recently characterized with the OTR screen at the AWA facility. These results indicates that the ZnTe crystal is suitable for use with this new wavelength at the specified location along the beamline.

FUTURE WORK

The remainder of the redesign is the detection of the 1550 nm light, which could be challenging. Silicon-based CCDs have a poor sensitivity in this wavelength range; while camera options exist, the prices are much higher. It is difficult to have three cameras for three measurement points as illustrated in Fig. 1. Alternatively, InGaAs linear array

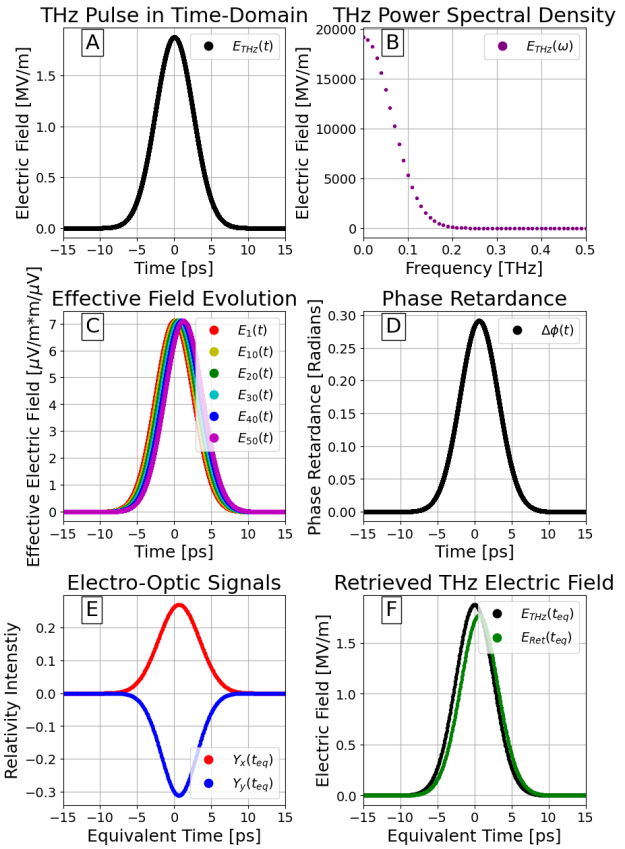

Figure 5: Simulation of 6 ps FWHM THz pulse retrieved via DEOS with the 1550 nm probe beam. A) THz pulse profile B) THz frequency components C) THz pulse propagation through 1 mm ZnTe accounting for group and phase velocity mismatch between the probe beam and the THz pulse D) Accumulated Phase Retardance $\Delta\phi(t)$ E) Electro-Optic Signals $Y_1(t_{eq})$ and $Y_2(t_{eq})$ and F) Retrieved THz profile via Maximum Ratio Combining method.

detectors could be implemented as Ref. [19], but commonly available linear array detectors have fewer number of detector elements than camera pixels, potentially lowering the resolution.

Additionally, depending on the detector sensitivity, a fiber amplifier may be needed to increase the stretched pulse's peak power to detectable levels. Also, if the gating capability of the detector is slow, we may require a pulse picker to ensure that only probe pulses synchronized with the THz pulse can be detected.

REFERENCES

[1] S. Casalbuoni, H. Schlarb, B. Schmidt, P. Schmüser, B. Steffen, and A. Winter, "Numerical Studies on the Electro-Optic Sampling of Relativistic Electron Bunches", in *Proc. PAC'05*, Knoxville, TN, USA, May 2005, paper RPAT049, pp. 3070–3072. doi:10.1109/pac.2005.1591367

[2] I. Wilke, A. M. MacLeod, W. A. Gillespie, G. Berden, G. M. H. Knippels, and A. F. G. van der Meer, "Single-Shot Electron-Beam Bunch Length Measurements", *Phys. Rev.*

ISBN: 978-3-95450-261-5 ISSN: 2673-7000 doi: 10.18429/JACoW-NAPAC2025-MOP026

Lett., vol. 88, no. 12, p. 124801, Mar. 2002. doi:10.1103/physrevlett.88.124801

[3] B. Steffen *et al.*, "Compact single-shot electro-optic detection system for THz pulses with femtosecond time resolution at MHz repetition rates", *Rev. Sci. Instrum.*, vol. 91, no. 4, p. 045123, Apr. 2020. doi:10.1063/1.5142833

[4] R. Roussel *et al.*, "Single Shot Characterization of High Transformer Ratio Wakefields in Nonlinear Plasma Acceleration", *Phys. Rev. Lett.*, vol. 124, no. 4, p. 044802, Jan. 2020. doi:10.1103/physrevlett.124.044802

[5] F. G. Sun, Z. Jiang, and X.-C. Zhang, "Analysis of terahertz pulse measurement with a chirped probe beam", *Appl. Phys. Lett.*, vol. 73, no. 16, pp. 2233–2235, Oct. 1998. doi:10.1063/1.121685

[6] X. Lu *et al.*, "Coherent high-power RF wakefield generation by electron bunch trains in a metamaterial structure", *Appl. Phys. Lett.*, vol. 116, no. 26, Jun. 2020. doi:10.1063/5.0012671

[7] K. L. F. Bane, P. Chen, and P. B. Wilson, "On Collinear Wake Field Acceleration", *IEEE Trans. Nucl. Sci.*, vol. 32, no. 5, pp. 3524–3526, Oct. 1985. doi:10.1109/tns.1985.4334416

[8] B. Jiang, C. Jing, P. Schoessow, J. Power, and W. Gai, "Formation of a novel shaped bunch to enhance transformer ratio in collinear wakefield accelerators", *Phys. Rev. Spec. Top. Accel Beams*, vol. 15, no. 1, p. 011301, Jan. 2012. doi:10.1103/physrevstab.15.011301

[9] T. Xu, "Precise Phase Space Control for Future Linear Colliders", Ph.D. dissertation, Northern Illinois University, De Kalb, IL, United States, 2022.

[10] Q. Gao *et al.*, "Observation of High Transformer Ratio of Shaped Bunch Generated by an Emittance-Exchange Beam Line", *Phys. Rev. Lett.*, vol. 120, no. 11, p. 114801, Mar. 2018. doi:10.1103/physrevlett.120.114801

[11] A. Zholents *et al.*, "A high repetition rate millimeter wavelength accelerator for an X-ray free-electron laser", *J. Instrum.*, vol. 20, no. 01, p. P01023, Jan. 2025. doi:10.1088/1748-0221/20/01/p01023

[12] G. Ha *et al.*, "Precision Control of the Electron Longitudinal Bunch Shape Using an Emittance-Exchange Beam Line", *Phys. Rev. Lett.*, vol. 118, no. 10, p. 104801, Mar. 2017. doi:10.1103/physrevlett.118.104801

[13] W. H. Tan, P. Piot, and A. Zholents, "Formation of temporally shaped electron bunches for beam-driven collinear wakefield accelerators", *Phys. Rev. Accel. Beams*, vol. 24, no. 5, May 2021. doi:10.1103/physrevaccelbeams.24.051303

[14] I. Kuzmin *et al.*, "Shaping triangular picosecond laser pulses for electron photoinjectors", *Laser Phys. Lett.*, vol. 16, no. 1, p. 015001, Nov. 2018. doi:10.1088/1612-202x/aaef95

[15] N. Majernik *et al.*, "Beam shaping using an ultrahigh vacuum multileaf collimator and emittance exchange beamline", *Phys. Rev. Accel. Beams*, vol. 26, no. 2, p. 022801, Feb. 2023. doi:10.1103/physrevaccelbeams.26.022801

[16] S. Kelham, G. Ha, P. Piot, and Y. Yang, "Progress towards longitudinal bunch profile monitor at the Argonne Wakefield Accelerator employing phase diversity electro-optic sampling", presented at IPAC'25, Taipei, Taiwan, Jun. 2025, paper THPM076, unpublished.

[17] F. Bienert, T. Graf, and M. A. Ahmed, "Designing of grating pulse compressors", *Biomed. Opt. Express*, vol. 33, no. 5, p. 11500, Mar. 2025. doi:10.1364/oe.554426

[18] J.-C. Diels, and W. Rudolph, *Ultrashort Laser Pulse Phenomena Fundamentals, Techniques, and Applications an a Femtosecond Time Scale*, Amsterdam, Netherlands: Academic Press, 1996.

[19] E. Roussel *et al.*, "Single-shot terahertz time-domain spectrometer using 1550 nm probe pulses and diversity electro-optic sampling", *Opt. Express*, vol. 31, no. 19, p. 31072, Sep. 2023. doi:10.1364/oe.498726